IR Absorption and Raman Spectra of Silicon Dioxide Nanoparticles in the Presence of Water: Computer Experiment

A. E. Galashev, O. R. Rakhmanova, and A. A. Borisikhin

Institute of Industrial Ecology, Ural Division, Russian Academy of Sciences,
ul. Sof'i Kovalevskoi 20-a, Yekaterinburg, 620219 Russia

Received November 11, 2009

Abstract—Interactions of $(SiO_2)_{50}$ clusters with 10, 20, 30, or 40 water molecules are studied by molecular dynamics method. Flat SiO_2 nanoparticle covered with a water layer is formed after the inclusion of water molecules into the cluster. As a rule, the integral intensity of IR and Raman spectra lowers after the absorption of H_2O molecules by the cluster. The power of IR radiation emitted by the cluster increases nonmonotonically with the addition of water molecules to the cluster. The absorption of water molecules by the cluster leads to a significant increase in the absorption coefficient and only a slight increase in the refractive index. The number of electrons participating in the interaction with electromagnetic radiation increases with the addition of water molecules to the cluster.

INTRODUCTION

Raman spectroscopy and IR absorption spectroscopy are common experimental tools for the identification of materials. The probing of oscillation dynamics provides extensive information on the mechanical and elastic properties of a material, as well as on occurring structural phase transitions. The theoretical determination of Raman and IR spectra serves as an additional powerful tool in experimental studies, particularly under extreme conditions when the experimental performance becomes more difficult. Theoretical analysis ensures a direct correlation between the positions of peaks observed in experimental spectra and the character of vibrations matching the atomic dynamics and the structure; it can be also used to accept or reject the structural models. Very often, the theoretical development in the simulation of the dynamics of vibrations in solids is confined to harmonic approximation. Theoretical models of IR and Raman spectra makes it necessary to calculate the derivative with respect to polarization vector and polarizability tensor over corresponding atomic displacements. Derivatives can be obtained from either simple empirical models or using quantum calculations based on ab initio principles. Harmonic approximation is best suited to the majority of solids at low temperatures. However, a large number of materials, including ferroelectrics, ionic conductors, and silicates, are subjected to order–disorder phase transitions upon changes in temperature and pressure. States that are realized in these states are completely anharmonic. Raman spectra of various metals, in particular liquid silicates in magma, have thus far been insufficiently interpreted theoretically. It is evident that harmonic approximations cannot describe such strongly anharmonic liquid phases. This problem can be fully solved when using molecular dynamics simulation when atomic displacements from equilibrium state can be arbitrarily large. According to the molecular dynamics simulation, the density of the state of oscillations can be calculated as the Fourier transformation of autocorrelation function of velocity, while derivatives with respect to polarization and polarizability can be calculated for every instantaneous configuration of a system over the course of its evolution. These calculations yield a complete description of the dynamics in anharmonic solids and liquids.

The first theoretical studies of interaction between water and silicon dioxide were focused on the calculations for gaseous clusters, which were incapable of to covering effects arising due to existence of bond network in a system [1–3]. Earlier calculations for a more voluminous system were concentrated on the diffusion of water into large quartz-like clusters, where the relaxation of only water molecules could take place [4]. The next step in considering the behavior of water in quartz was the study of the response of bond network in large quartz-like clusters [5]. The diffusion and response of water on the presence of defects and rings with different sizes in silicon dioxide were studied quite recently [6, 7]. The existence of activation barriers and the region of relative stability between molecular water and silanol states, i.e., the existence of structures of Si–OH type, was revealed in these works. The presence of water in silicon dioxide in both the molecular form and the form of silanol groups greatly affects its physical properties. At low temperatures, the presence of water considerably affects the

optical characteristics of SiO_2.. Experiments give evidence of the exchange between oxygen isotopes of labeled water and the network formed by silicon dioxide [8, 9]. The dependence of water solubility in silicon dioxide on the temperature and pressure of water vapor was disclosed in [10]. A considerable relaxation of the bond network caused by the reaction between water and SiO_2 on the surface and in the bulk of semiconductor was revealed experimentally [11, 12]. The response of bond network to the reaction between water and SiO_2 in bulk amorphous and crystalline silicon dioxide was also studied by the density functional [13]. High reactivity of the node and low activation barrier are associated with high-stress state, in which the silanol state is stabilized to a great extent by the relaxation of bond network.

Molecular dynamics model enables us to study in detail the mechanism of the adsorption of molecules. Complete physical and chemical picture of the penetration of water into silicon dioxide remains so far scarcely studied. Systematic studies of the effect of different portions of water on $(SiO_2)_n$ clusters seem to be interesting. These clusters can be used to study the effects of solvent or to identify the local structure of amorphous SiO_2.

The goal of this work is to study the adsorption of water molecules by a silicon dioxide cluster; to investigate the effect of the addition of water molecules on the IR absorption and Raman spectra caused by the $(SiO_2)_n$ cluster, as well as on the number of electrons that participate in the interaction with electromagnetic radiation.

INTERACTION POTENTIALS

To describe the pair part of interactions in the SiO_2 system, we used the Morse–Stretch potential [14]

$$\Phi(r_{ij}) = \frac{q_i q_j}{r_{ij}} + \\ + D_{ij}\left\{\exp\left[\gamma_{ij}\left(1 - r_{ij}/r_{ij}^0\right)\right] - 2\exp\left[\frac{\gamma_{ij}}{2}\left(1 - r_{ij}/r_{ij}^0\right)\right]\right\}, \quad (1)$$

where interaction between i th and j th atoms is governed by parameters $q_j, D_{ij}, \gamma_{ij}, r_{ij}^0$ (see Table 1 in [14]), as well as distance r_{ij} between atoms. This form of potential was derived from the Born–Mayer potential. Potential (1) describes transitions between different phases. This potential is cut off at a distance of 0.9 nm. It is known that potentials of type (1) are diverged at short distances. Therefore, their use can be problematic at high temperatures and pressures. In addition to pair potential, the effects of dipole polarization were included. The polarizability $\alpha^{(p)} = 3.219$ Å corresponding to the experimental value of the polarizability of SiO_2, molecule was referred to the center of mass

of this structural unit. The Si–O length in this structural unit corresponded to the least distance $r_{Si-O} = 0.162$ nm in the crystal of α-quartz; the O–Si–O angle was equal to tetrahedral angle 109.5°.

The description of interactions of water molecules in the model is based on the modified TIP4P interaction potential and rigid four-center model of H_2O molecule [15]. The modification of interaction potential for water involved changes in the parameters of the Lennard-Jones part of potential and the localization of the negative charge. As a result, the permanent dipole moment for the water molecule became equal to its experimental value of 1.848 D. The geometry of this molecule corresponds to the experimental parameters of a molecule in the gaseous state: $r_{OH} = 0.09572$ nm and the H–O–H angle $= 104.5°$ [16]. Fixed charges ($q_H = 0.519e$, $q_M = -1.038e$) are attributed to H atoms and point M on the bisectrix of H–O–H angle at a distance of 0.0215 nm from oxygen atom. Values of charges and the position of point M are chosen to reproduce experimental values of dipole and quadrupole moments [17, 18], as well as the values of the energy of dimer and its characteristic distances calculated form ab initio principles [19]. The stabilization of short-range order in water clusters is achieved mainly due to the Lennard-Jones short-range potential with interaction center assigned to oxygen atom. In addition to electric charge, the polarizability (1.49 Å^3) [20], which is required to describe nonadditive polarization energy, is also assigned to point M. Standard iterative technique was used to calculate induced dipole moments at each time step [15]. The accuracy of determining $\mathbf{d}_i$ is set within the $10^{-5}-10^{-4}$ D range.

Atom–atom SiO_2–H_2O interactions were preset via the sum of repulsive, dispersive, and Coulombic contributions

$$\Phi(r_{ij}) = b_i b_j \exp\left[-(c_i + c_j)r_{ij}\right] - a_i a_j r_{ij}^{-6} + \frac{q_i q_j}{r_{ij}},$$

where potential parameters a_i, b_i, c_i that describes these interactions were taken from [21].

MOLECULAR DYNAMICS MODEL

We considered flexible models of molecules. The flexibility of molecules was created using the procedure developed on the basis of Hamiltonian dynamics [22, 23]. Let atoms a and b in a molecule be separated by the distance

$$q = |\mathbf{r}_a - \mathbf{r}_b|,$$

where $\mathbf{r}_a$ and $\mathbf{r}_b$ are vectors that determine the positions of atoms. Corresponding velocities are denoted by $\mathbf{v}_a$

and $\mathbf{v}_b$, and the reduced mass is written in its usual form

$$\mu = \frac{m_a m_b}{m_a + m_b}.$$

The size of molecule presented by atoms a and b is determined by the balance between total potential $\mathbf{f}(\mathbf{q}) = -\dfrac{\partial \mathbf{r}}{\partial \mathbf{q}} \nabla \Phi(\mathbf{r})$ and centrifugal $-\mu q \omega^2$, forces so that

$$-\mu q \omega^2 - \mathbf{f}(\mathbf{r}) \frac{\partial \mathbf{r}}{\partial \mathbf{q}} = 0,$$

where $\omega = |\mathbf{v}_a - \mathbf{v}_b|/q$ is the angular velocity. From the minimization of contributions to potential energy U from each generalized coordinate, we arrive at

$$\frac{\partial}{\partial q_i} H(\mathbf{r}, \mathbf{v}) = \frac{\partial}{\partial q_i} \left(\frac{1}{2} \mu_i q_i^2 \omega_i^2 + U(\mathbf{r}) \right) = 0.$$

This method can easily be generalized to the molecules of any composition [24].

Flexible Si−O bond in the silicon dioxide nanoparticle can be ruptured and oxygen atoms tend to reach the particle surface [25]. This model suggests the rupture of Si−O bond when its length increases (with respect to initial bond in SiO_4 tetrahedron) by more than 20%. The detachment of oxygen atoms and the formation of silicon clusters (composed of a few atoms) can be related to the formation of nonequilibrium defect structure in the course of the synthesis of silicon dioxide nanoparticles. At low temperature, the bond can be ruptured due to the penetration of water into loose tetrahedron-coordinated structure of silicon dioxide nanoparticle. In the case when the internal (with the structure similar to that of material bulk) and peripheral parts can be isolated, the enrichment of surface with oxygen due to the effect of H_2O molecules can be identified as cooperative effect. The formation of larger silicon clusters (nanoclusters) in silicon dioxide occurs under the effect of electron beam by virtue of the local overheating of irradiated microvolume. According to momentum conservation law, the electron cannot transfer the energy to silicon or oxygen atoms that is sufficient to rupture Si−O bond. Correspondingly, the main reason for the formation of silicon nanoclusters is the local overheating of the microvolume in silicon dioxide.

Initial filling of the space with SiO_4 tetrahedra, which act as a base for the formation of silicon dioxide nanoparticle $(SiO_2)_{50}$, was achieved using GRINSP software [26]. In the configuration composed of SiO_4, tetrahedra, structural SiO_2 units were identified. Initial velocities for SiO_2 particles were set randomly; they were adjusted to the temperature of 293 K by the division of injected or released thermal energy in proportion to velocity modulus. Afterwards, we preliminarily calculated the molecular dynamics for 50 struc-

tural SiO_2, units combined into a cluster. The duration of this calculation was 10^6 time steps $\Delta t = 10^{-16}$ s. Over this period of time, the studied system maintained the equilibrium state, which was confirmed by the establishment of the Maxwell velocity distribution of SiO_2 objects. In this case, the structure of the nanoparticle relaxed to energy-favorable packing ($U \approx -0.9$ eV/particle). Then, at a time instant taken as zero time ($t = 0$), water molecules were introduced into the environment of the $(SiO_2)_{50}$ nanoparticle. For this purpose, the sphere was drawn from the center of cluster mass, which can contain up to 40 water molecules. The centers of mass and orientation of molecules were set by random number generator. The radius of sphere is equal to ~2.0 nm; the distances between the centers of mass of added molecules, as well as between H_2O molecules and structural SiO_2 units, were no shorter than 0.55 nm. Water molecules could occupy internal cavities in the $(SiO_2)_{50}$. cluster. Four calculations were performed with different numbers N_w of water molecules surrounding the $(SiO_2)_{50}$, nanoparticle ($N_w = 10$, 20, 30, and 40). In each case, the main calculations were preceded by preliminary calculations with a duration of $0.5 \times 10^6 \Delta t$ accompanied by the necessary structural relaxation of a system related to the reorientation and changes in the positions of triatomic SiO_2 elements and water molecules. The main calculation for determining spectral characteristics of a system composed of $(SiO_2)_{50}$ cluster and water molecules was equal to $2.5 \times 10^6 \Delta t$. We determine the studied systems as follows: I $(SiO_2)_{50}$, II $(H_2O)_{10}(SiO_2)_{50}$, III $(H_2O)_{20}(SiO_2)_{50}$, IV $(H_2O)_{30}(SiO_2)_{50}$, and V $(H_2O)_{40}(SiO_2)_{50}$.

The motion equations for the centers of mass of structural units and molecules were integrated by the Gear fourth-order method [27]. Equations for the rotational motion of structural units (molecules) were analytically solved using the Rodrigo−Hamilton parameters [28]. The integration scheme for rotational motion equations corresponded to the approach proposed by Sonnenschein [29]. The calculations were carried out with a Pentium-IV four-quad computer at a processor clock frequency of 2.83 GHz.

DIELECTRIC PROPERTIES

The total dipole moment of a system, $\mathbf{d}_{cl}$, was calculated by the formula

$$\mathbf{d}_{cl}(t) = Z_+ \sum_{i=1}^{N_{tot}^+} \mathbf{r}_i(t) + Z_- \sum_{i=1}^{N_{tot}^-} \mathbf{r}_i(t),$$

where $\mathbf{r}_i(t)-$ is the vector indicating the positions of i th atom or point M at time instant t and Z is the electric charge in the considered center; subscript "+" refers

to H or Si atoms carrying positive electric charge, whereas subscript "−" refers to point M or oxygen atoms in the massive SiO_2, N_{tot}^+ and N_{tot}^- are the number of positive and negative charges in a system, respectively.

Permittivity $\varepsilon(\omega)$ as a function of frequency ω was represented as complex value $\varepsilon(\omega) = \varepsilon'(\omega) - i\varepsilon''(\omega)$, which was defined by the equation [30, 31]

$$\frac{\varepsilon(\omega) - 1}{\varepsilon_0 - 1} = -\int_0^\infty \exp(-i\omega t)\frac{dF}{dt}dt =$$

$$= 1 - i\omega\int_0^\infty \exp(-i\omega t)F(t)dt,$$

where the $F(t)$ function is the normalized autocorrelation function of the total dipole moment of cluster

$$F(t) = \frac{\langle \mathbf{d}_{cl}(t)\cdot\mathbf{d}_{cl}(0)\rangle}{\langle \mathbf{d}_{cl}^2\rangle}.$$

The cross section of the absorption of IR radiation is set as follows [32]:

$$\sigma(\omega) = \left(\frac{2}{\varepsilon_0 c\hbar\eta}\right)\omega \,\mathrm{th}\left(\frac{\hbar\omega}{2kT}\right)\mathrm{Re}\int_0^\infty dt e^{i\omega t}\langle \mathbf{M}(t)\mathbf{M}(0)\rangle,$$

where $\hbar$ is the Planck constant, η is the refractive index, ε_0 is the electric constant, and c is the speed of light.

In the case of depolarized light, the Raman spectrum $J(\omega)$ is set by expression [32]

$$J(\omega) = \frac{\omega}{(\omega_L - \omega)^4}\left(1 - e^{-\hbar\omega/kT}\right)\mathrm{Re}\int_0^\infty dt e^{i\omega t}\langle \Pi_{xz}(t)\Pi_{xz}(0)\rangle,$$

where

$$\Pi(t) \equiv \sum_{j=1}^N \left[\alpha_j^{(p)}(t) - \langle\alpha_j^{(p)}\rangle\right],$$

ω_L) is the frequency of exciting laser, Π_{xz} presents the xz-component of $\Pi(t)$, value, the x-axis is directed along the molecular dipole, and the xy plane is the molecular plane of water molecule. In the simulation, we used value $\omega_L = 19\,436.3$ cm^{-1} (the green line of an argon laser; $\lambda = 514.5$ nm).

The frequency dispersion of permittivity determines the frequency dependence of dielectric losses $P(\omega)$ in accordance with the expression [33]

$$P = \frac{\varepsilon''\langle E^2\rangle\omega}{4\pi},$$

where $\langle E^2\rangle$ is the average value of the square of electric field strength and ω) is the frequency of emitted electromagnetic wave.

The total number of electrons N_e in the unit volume of cluster interacting with external electromagnetic field is set as [31]

$$N_{el} = \frac{m}{2\pi^2 e^2}\int_0^\infty \omega\varepsilon''(\omega)d\omega,$$

where e and m are the charge and mass of electron, respectively.

Refractive index η and absorption coefficient ξ of medium are defined by the expressions [34]

$$\eta = \sqrt{\frac{\varepsilon' + \sqrt{\varepsilon'^2 + \varepsilon''^2}}{2}}, \quad \xi = \sqrt{\frac{-\varepsilon' + \sqrt{\varepsilon'^2 + \varepsilon''^2}}{2}}.$$

Coefficient ξ determines the rate of wave decay with its propagation in the medium.

RESULTS OF CALCULATIONS

The configurations of $(H_2O)_{30}(SiO_2)_{50}$ cluster at time instants $t = 0$ and 250 ps are shown in Fig. 1. At the initial time instant, H_2O molecules filled the cavities in the $(SiO_2)_{50}$. cluster. However, this structure turned out to be unstable. Loose nanoparticle of silicon dioxide tends to form a closely packed layered structure even in the absence of water molecules. This tendency is conserved in the presence of water. Moreover, water molecules play essentially the role of equal partners of structural SiO_2, units; i.e., they create a layered structure with these units. The specificity of this rearrangement is that the structural unit of each type tends to combine with similar unit, which leads to the formation of superimposing monolayers of silicon dioxide and water. However, the SiO_2 layers grow more quickly, which is evidenced by higher values of self-diffusion coefficients of structural SiO_2. units. This can be explained by the appearance of the SiO_2 island in the uppermost layer (Fig. 1b) formed by water molecules. The formation of layered structure for $(H_2O)_i(SiO_2)_{50}$ clusters resulted in the disintegration of construction built from SiO_4. tetrahedra. At a small amount of SiO_4 tetrahedra, the detachment of oxygen atoms, i.e., the rupture of an Si−O bond, becomes energy unfavorable. Low temperature (293 K) also promotes the conservation of structural SiO_2 units in the course of simulation.

Frequency dependences of real and imaginary parts of permittivity are presented in Fig. 2. Both dependences are changed substantially after the absorption of water molecules by $(SiO_2)_{50}$ cluster. The $\varepsilon'(\omega)$ function for the $(SiO_2)_{50}$ cluster has the maximum in the vicinity of the frequency $\omega = 182$ cm^{-1}. Generally, the $\varepsilon'(\omega)$ function for this cluster decreases with further increase in the frequency passing another two diffuse maxima at frequencies of 490 and 795 cm^{-1}. After the absorption of 10 to 40 water mole-
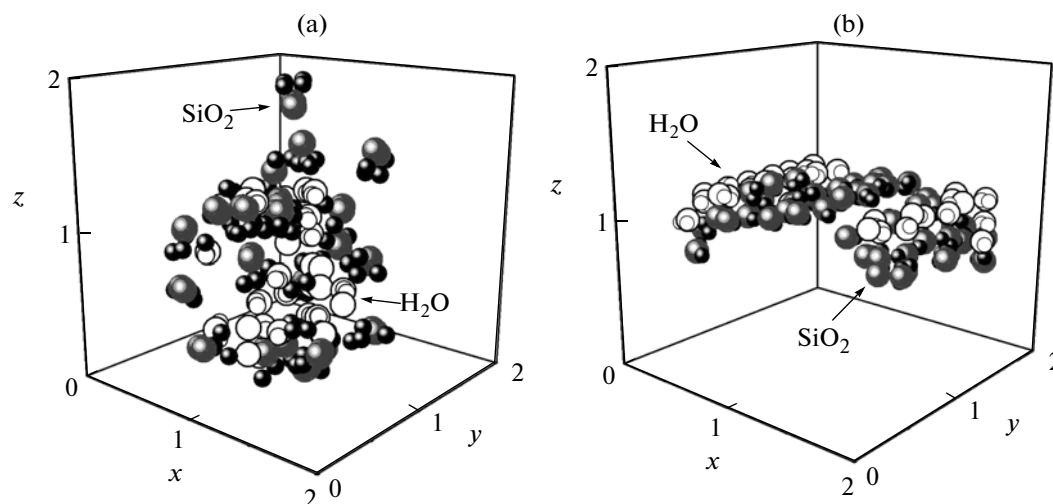
Fig. 1. Configurations of $(H_2O)_{30}(SiO_2)_{50}$ nanoparticle corresponding to time instants (a) 0 and (b) 250 ns. Coordinates of molecules are presented in nm.

cules by the cluster, the $\varepsilon'(\omega)$ functions increase over the $30 \leq \omega \leq 900$ cm^{-1} range. Moreover, in these cases, the maximum of $\varepsilon'(\omega)$ function falls on the frequency $\omega = 916$ cm^{-1}, i.e., the position of the maximum does not vary depending on the number of absorbed molecules. The presence of water in the cluster, makes the values of $\varepsilon'(\omega)$ function larger at frequencies exceeding 270 cm^{-1}. The $\varepsilon'(\omega)$ function for liquid water [35] rapidly decreases with increasing frequency (Fig. 2a, curve 6) without any oscillations.

The absorption of water molecules by the $(SiO_2)_{50}$ cluster leads even to greater changes in the frequency dependence of the imaginary part of permittivity. All of the obtained $\varepsilon''(\omega)$ functions (up to ≈ 830 cm^{-1}) are increasing functions; however, the presence of water molecules in the cluster smoothes oscillations of these functions. On average, after the absorption of even ten water molecules by the cluster, the values of $\varepsilon''(\omega)$ function increased by 1.46 times and continue to increase with the number of absorbed water molecules. In general, the capture of water molecules by the $(SiO_2)_{50}$ cluster shifts the position of the principal maximum of $\varepsilon''(\omega)$ function toward the region of low frequencies, except for the case of the absorption of 40 water molecules, when the position of the principal peak remains almost unchanged. The $\varepsilon''(\omega)$ function for liquid water [36] decreases with increasing frequency accompanied by large oscillations (Fig. 2b, curve 6). The positions of local maxima of this function fall on frequencies of 145 and 520 cm^{-1}. At $\omega > 210$ cm^{-1}, the values of $\varepsilon''(\omega)$ function for liquid water become lower than corresponding functions for silicon dioxide cluster; at $\omega > 607$ cm^{-1}, they are lower than for the $(SiO_2)_{50}$ cluster.

IR absorption spectra for clusters are shown in Fig. 3. The $\sigma(\omega)$ spectra for bulk solid α-quartz (curve 6) and liquid water (curve 7) are also presented
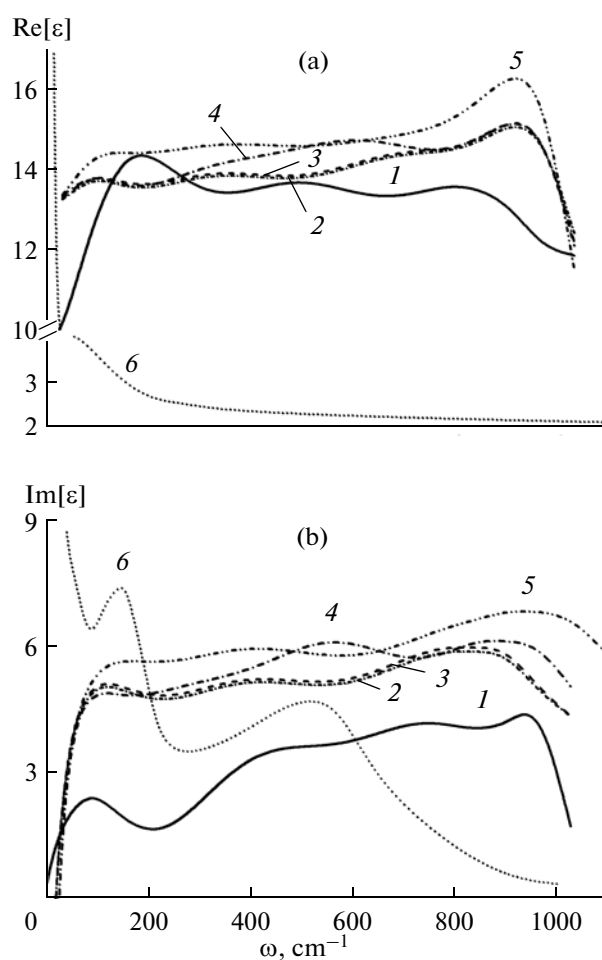
Fig. 2. Dependences of (a) real and (b) imaginary parts of permittivity on frequency for (1–5) systems I–V; (5) (a) MD calculation for massive liquid water [35] and (b) experimental data for liquid water [36].
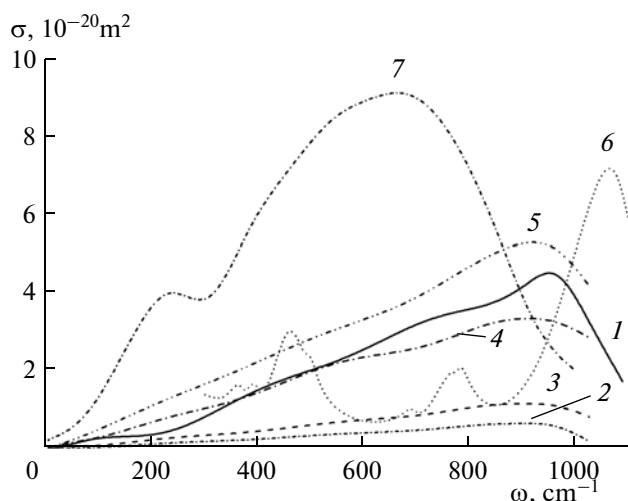
Fig. 3. IR absorption spectra for systems formed by $(SiO_2)_{50}$ cluster and water molecules: (*1–5*) systems I–V, (*6*) experimental spectrum of α-quartz at 300 K [37], and (*7*) experimental spectrum of liquid water at 293 K [38].
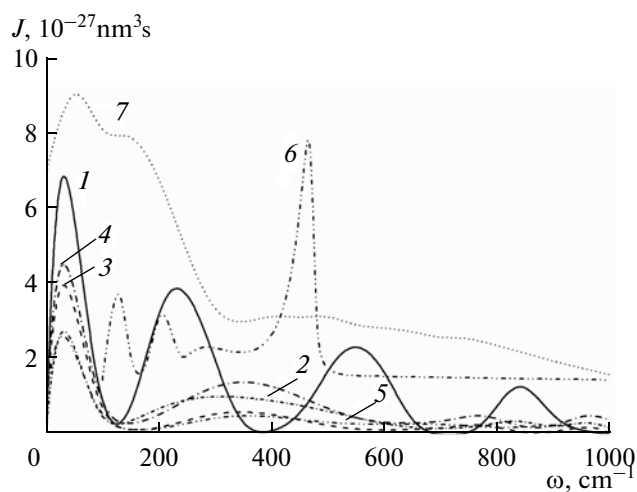
Fig. 4. Raman spectra for systems formed by $(SiO_2)_{50}$ cluster and water molecules: (*1–5*) systems I–V, (*6*) experimental spectrum of α-quartz at 300 K [37], and (*7*) experimental spectrum of liquid water at 293 K [39].

in this figure for comparison. It can be seen that the integral intensities of IR spectra are varied markedly with the absorption of water molecules by the $(SiO_2)_{50}$ cluster. When the cluster contains 10–30 water molecules, the values of corresponding $\sigma(\omega)$ functions are generally lower than the $\sigma(\omega)$ function for the $(SiO_2)_{50}$ cluster. However, when the number of absorbed molecules in the cluster becomes equal to 40, its IR spectrum acquires larger integral intensity than the $\sigma(\omega)$ spectrum of the cluster of pure silicon dioxide. Lower intensity of IR spectrum after the absorption of 10–30 water molecules by the cluster is related to the weakening of Si–O bonds due to the pulling of oxygen atoms of silicon dioxide by hydrogen atoms of water molecules. In view of the fact that, in this case, the number of water molecules is relatively small, the relevant contribution to the IR spectrum of the cluster becomes insufficient to compensate for the weakening of Si–O bonds. However, as the number of absorbed water molecules increases, their contribution to the IR spectrum of the cluster becomes more and more perceptible. Finally, after the absorption of 40 water molecules by the cluster, the integral intensity of the IR spectrum of $(H_2O)_{40}(SiO_2)_{50}$ cluster becomes higher than corresponding characteristic for $(SiO_2)_{50}$ cluster. The $\sigma(\omega)$ spectra of clusters have one maximum whose position is shifted toward the region of low frequencies after the absorption of water molecules by the cluster. The position of the maximum of IR spectrum for clusters is intermediate between the values corresponding to positions of principal maxima in $\sigma(\omega)$ spectra of solid α-quartz and liquid water. In the IR spectrum of solid α-quartz [37], along with principal maximum at $\omega = 1065$ cm^{-1}, additional peaks are observed at 460 and 783 cm^{-1}, whereas, in the $\sigma(\omega)$ spectrum of liquid

water, the peak is localized at 200 cm^{-1}1 before the principal maximum at $\omega = 690$ cm^{-1} [38].

Raman spectra $J(\omega)$ for nanoparticles are shown in Fig. 4. It can be seen that the absorption of water molecules by the $(SiO_2)_{50}$ cluster considerably changes its Raman spectrum. The $J(\omega)$ spectrum is transformed from strongly oscillating (for $(SiO_2)_{50}$ nanoparticle) to diffuse smooth spectrum for silicon dioxide nanoparticles containing water. The principal maximum of $J(\omega)$ spectrum at 33 cm^{-1} does not change its position; however, the spectrum becomes less intense in the presence of water. The following ratios were obtained between the intensities of the first peak of $J(\omega)$ spectra for systems I–V: 1 : 0.40 : 0.56 : 0.63 : 0.35, respectively. Thei nitial drop in the intensity of the first peak related to the absorption of H_2O molecules is restored with an increase in the amount of water molecules in a system. The intensity and position of the second peak of $J(\omega)$ spectrum are very sensitive to variations in the quantitative composition of $(H_2O)_i(SiO_2)_{50}$ cluster. Subsequent peaks are resolved weakly and change their positions with the variations in the number of water molecules in a system. Figure 4 demonstrates also experimental Raman spectra of bulk silicon dioxide [37] (curve *6*) and water (curve *7*) [39]. Principal maxima of these spectra are localized at 467 and 56 cm^{-1}, respectively. The second peaks of $J(\omega)$ spectra for studied nanoparticles are located between these values. The reciprocal half-width of peaks of Raman spectra characterizes the lifetime τ of IR phonons. As can be seen from obtained $J(\omega)$ spectra, time τ essentially (up to two times) decreased after the absorption of water molecules by the $(SiO_2)_{50}$ nanoparticle.

The power of IR radiation emitted by the silicon dioxide cluster changes nonmonotonically with the

P, 10^{-4} W/cluster
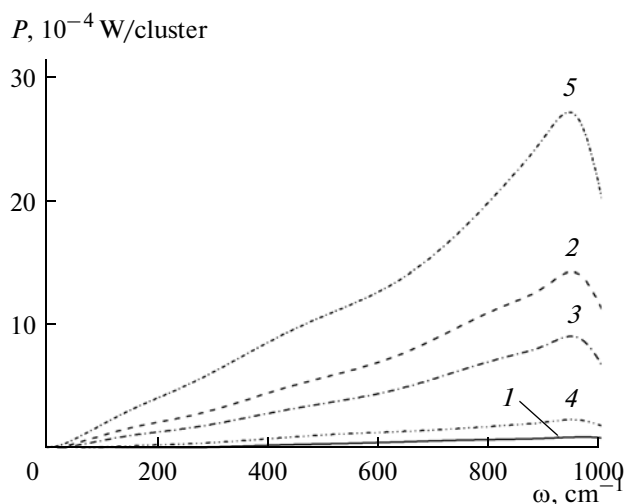
Fig. 5. IR emission spectra for $(H_2O)_i(SiO_2)_{50}$ clusters, $i = 0-40$: *1–5* systems I–V.

N_{el}, 10^{14} 1/cm^3

Fig. 6. Dependence of number of electrons in $(H_2O)_i(SiO_2)_{50}$ clusters interacting with external electromagnetic radiation on number of absorbed water molecules.

addition of water molecules to the nanoparticle. The $P(\omega)$ spectra for studied systems are shown in Fig. 5. In all considered cases, the absorption of water molecules significant increases the power of radiation emitted by the cluster. Integral intensities of $P(\omega)$ spectra for systems I–V are in the 1 : 13.7 : 8.7 : 2.4 : 25.2 ratio. The significant increase in the intensity of $P(\omega)$ spectrum is explained by the addition of polar H_2O molecules with a large permanent dipole moment.

The dependence of number N_{el} of electrons active to electromagnetic radiation on the amount of H_2O molecules absorbed by the $(SiO_2)_{50}$ nanoparticle is shown in Fig. 6. According to this figure, the N_{el} value increases with the number of water molecules in the nanoparticle. The N_{el} value rapidly increases due to the addition of even 10 water molecules to $(SiO_2)_{50}$ cluster. The number of active electrons increases by 1.65 times, whereas the number of water molecules in the nanoparticle increases to 40 molecules. An increase in the N_{el} value correlates with the rise in the integral intensity of the absorption of IR radiation by nanoparticles; albeit, it does not crucially affect their Raman spectra.

The absorption coefficient (Fig. 7) for $(SiO_2)_{50}$ cluster is a decreasing function within the larger part of the $0 \leq \omega \leq 1000$ cm^{-1} range and refractive index (Fig. 8) is an increasing function. For $(H_2O)_i(SiO_2)_{50}$, i clusters, $\xi(\omega)$ and $\eta(\omega)$ functions rapidly increase in the beginning of frequency range until ω reaches the value of 100 cm^{-1}. These values then increase slightly up to the frequency of ≈ 900 cm^{-1}. The principal maximum of coefficient ξ for these clusters lies within the narrow $930 \leq \omega \leq 940$ cm^{-1} frequency range. Weakly pronounced principal maximum of coefficient η fits the $920 \leq \omega \leq 940$ cm^{-1} range. Curves *6* in Figs. 7 and 8
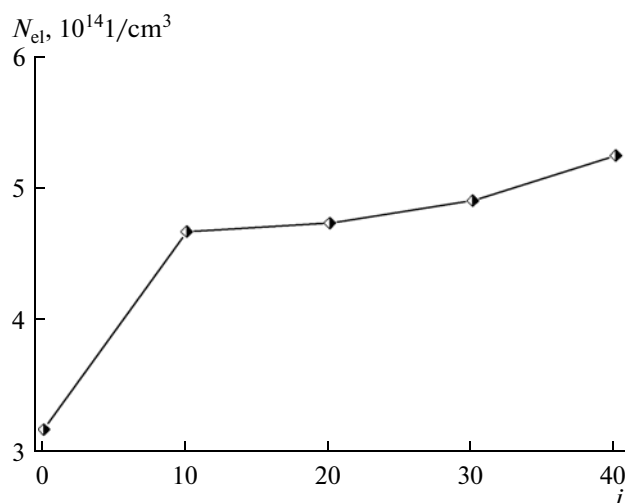
indicate $\xi(\omega)$ and $\eta(\omega)$ functions for the massive glass of silicon dioxide calculated from experimental IR absorption spectrum using Kramers–Kroning relations [40]. In the $0 \leq \omega \leq 1000$ cm^{-1} range, the $\xi(\omega)$ spectrum for massive SiO_2 glass is characterized by four peaks, while $\eta(\omega)$ function is characterized by oscillations. On average, coefficient ξ for silicon dioxide clusters are 1.17-fold larger than for SiO_2, glass; coefficient η for the cluster is also 1.8-fold larger. This ratio between the values of $\xi(\omega)$ and $\eta(\omega)$ functions in the cluster and massive glass can be attributed to the surface curvature of nanoparticle. Experimental $\eta(\omega)$ dependence for liquid water is smooth decreasing function (curve *7*) [41].
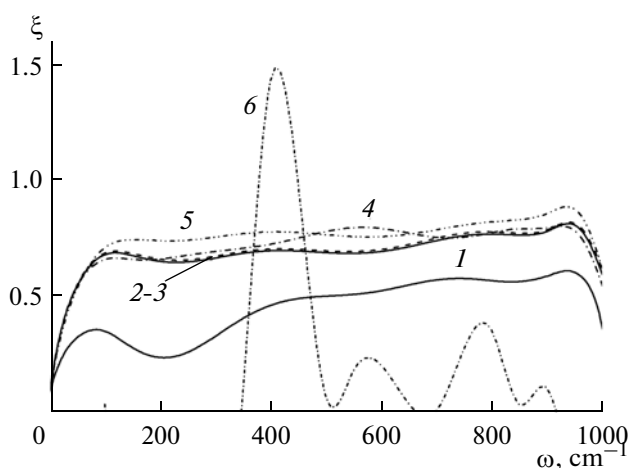
Fig. 7. Frequency dependences of absorption coefficient: (*1–5*) systems I–V and (*6*) coefficient ξ for SiO_2 glass [40].
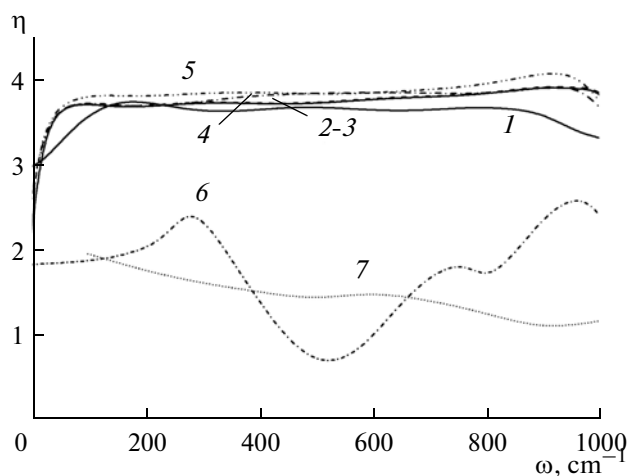
Fig. 8. Frequency dependences of refractive index: (*1*−5) systems I–V, (*6*) coefficient η for SiO_2 [40], glass [40], and (*7*) for liquid water, experiment [41].

CONCLUSIONS

The behavior of water flown inside the silicon dioxide nanoparticle was investigated without the participation in the reaction led to the formation of silanol group was studied. The absence of chemical hindrances for moving water molecules throughout the volume of $(SiO_2)_{50}$ nanoparticle facilitated the formation of layered structure in which water is spread over the SiO_2, surface. Moreover, in this process, the formation of SiO_2 layers outstrips the growth of water layers. Changes in the structure and composition of nanoparticle affected its dielectric and optical properties. The first effect of the interaction between water and $(SiO_2)_{50}$ cluster was a decrease in the intensity of IR absorption spectra. However, as the concentration of water in the nanoparticle increases, the intensity of this spectrum rose and exceeded that of initial cluster when the number of water molecules achieved 40. The capture of water molecules by silicon dioxide cluster significantly changes its Raman spectrum that is expressed in a decrease in the integral intensity and smoothing of spectrum form. The lowest intensity of Raman spectrum was observed for the nanoparticle that attached 40 water molecules. The power of IR radiation emitted by the cluster always increased in the presence of water molecules in the cluster. The power of radiation could be lowered with an increase in the concentration of water in the cluster; however, when the cluster absorbed 40 water molecules, the power of emission was the highest. The absorption of water does not greatly change the optical characteristics of $(SiO_2)_{50}$ nanoparticle. The absorption coefficient and refractive index varied slightly within wide frequency range that differ substantially their frequency dependence from the behavior of analogous properties of silicon dioxide glass.

The formation of Si−O_W bonds (where O_W is the water oxygen) resulted in the gain in energy. However, the network of S−O bonds in silicon dioxide is distorted in this case; i.e., stresses in the bond network formed by Si and O atoms are induced, thus causing the same energy consumption as for the formation of Si−O_W bonds. If the sizes of cavities in silicate glass are smaller than 0.45−0.50 nm, the energy of the inclusion of water molecule into such cavity turned out to be high, at least higher than 1 eV. In contrast to silicate glass, the network of Si−O bonds in silicon dioxide nanoparticle is more flexible and less strong, because the nanoparticle has lower density than glass. Because of this, the penetration of water molecule through the network of Si−O bonds in silicon dioxide nanoparticle proceeds much easier and faster than in the glass. Upon the formation of Si−O_W bonds in the glass, electric charge is transferred between protons of water molecule entering into the cavity and the network of oxygen atoms participating in hydrogen bonding with water molecule. Charges on oxygen atoms of water and SiO_2, vary in the course of the formation of silanol groups. Slight change is observed for hydrogen atom participating in the formation of hydrogen bonds. Silicon atoms are characterized by much larger (~0.1e) fluctuations of electric charge. In a simplified model used in this work, these phenomena were not taken into account. More precise model should also accounted for changes in the pattern of interaction potential, when the bonds between different molecular components are formed or ruptured. Moreover, the role of polarization and higher electric moments in the formation of silanol groups should be investigated in more detail.

REFERENCES

1. Uglienko, P., Saunders, V., and Garrone, E., *J. Phys. Chem.*, 1990, vol. 94, p. 2260.
2. Lasaga, A.C. and Gibbs, G.V., *Am. J. Sci.*, 1990, vol. 290, p. 263.
3. Heggie, M. and Jones, R., *Philos. Mag. Lett.,* 1987, vol. 55, p. 47.
4. Hagon, J.P., Stoneham, A.M., and Jaros, M., *Philos. Mag. B*, 1987, vol. 55, p. 225.
5. Jones, R., Oberg, S., Heggie, M.I., and Tole, P., *Philos. Mag. Lett.*, 1992, vol. 66, p. 61.
6. Bakos, T., Rashkeev, S.N., and Pantelides, S.T., *Phys. Rev. Lett.*, 2002, vol. 88, p. 05508.
7. Bakos, T., Rashkeev, S.N., and Pantelides, S.T., *Phys. Rev. B: Condens. Matter*, 2004, vol. 69, p. 195206.
8. Drury, T. and Roberts, J.P., *Phys. Chem. Glasses*, 1963, vol. 4, p. 79.
9. Mikkelsen, J.C., *Appl. Phys. Lett.*, 1981, vol. 39, p. 903.
10. Roberts, G.J. and Roberts, J.P., *Phys. Chem. Glasses*, 1964, vol. 5, p. 26.
11. Tomozawa, M., Li, H., and Davis, K.M., *J. Non-Cryst. Solids*, 1994, vol. 179, p. 162.

12. Davis, K.M. and Tomozawa, M., *J. Non-Cryst. Solids*, 1995, vol. 185, p. 203.

13. Van Ginhoven, R.M., Jonsson, H., Park, B., and Corrales, L.R., *J. Phys. Chem. B*, 2005, vol. 109, p. 10936.

14. Tangney, P. and Scandolo, S., *J. Chem. Phys.*, 2002, vol. 117, p. 8898.

15. Dang, L.X. and Chang, T.-M., *J. Chem. Phys.*, 1997, vol. 106, p. 8149.

16. Benedict, W.S., Gailar, N., and Plyler, E.K., *J. Chem. Phys.*, 1956, vol. 24, p. 1139.

17. Xantheas, S., *J. Chem. Phys.*, 1996, vol. 104, p. 8821.

18. Feller, D. and Dixon, D.A., *J. Phys. Chem.*, 1996, vol. 100, p. 2993.

19. Smith, D.E. and Dang, L.X., *J. Chem. Phys.*, 1994, vol. 100, p. 3757.

20. *Spravochnik khimika* (Chemist's Handbook), Nikol'skii, B.P., Ed., Leningrad: Khimiya, 1971 vol. 1.

21. Spackman, M.A., *J. Chem. Phys.*, 1986, vol. 85, p. 6579.

22. Lemberg, H.L. and Stillinger, F.H., *J. Chem. Phys.*, 1975, vol. 62, p. 1677.

23. Rahman, A., Stillinger, F.H., and Lemberg, H.L., *J. Chem. Phys.*, 1975, vol. 63, p. 5223.

24. Saint-Martin, H., Hess, B., and Berendsen, H.J.C., *J. Chem. Phys.,* 2004, vol. 120, p. 11133.

25. Galashev, A.E. and Skokov, V.N., *Teplofiz. Vys. Temp.*, 2003, vol. 41, p. 386.

26. Le Bail, A., *J. Appl. Crystallogr.*, 2005, vol. 38, p. 389.

27. Haile, J.M., *Molecular Dynamics Simulation. Elementary Methods*, New York: Wiley, 1992.

28. Koshlyakov, V.N., *Zadachi dinamiki tverdogo tela i prikladnoi teorii giroskopov* (Prioblems of Solid Body Dynamics and the Applied Theory of Gyroscopes), Moscow: Nauka, 1985.

29. Sonnenschein, R., *J. Comput. Phys.*, 1985, vol. 59, p. 347.

30. Bresme, F., *J. Chem. Phys.*, 2001, vol. 115, p. 7564.

31. Neumann, M., *J. Chem. Phys.*, 1985, vol. 82, p. 5663.

32. Bosma, W.B., Fried, L.E., and Mukamel, S., *J. Chem. Phys.*, 1993, vol. 98, p. 4413.

33. *Fizicheskaya entsiklopediya* (Physical Encyclopedia), Prokhorov, A.M., Ed., Moscow: Sovetskaya Entsiklopediya, 1988, vol. 1, p. 702.

34. Landau, L.D. and Lifshitz, E.M., *Electrodynamics of Continuous Media*, Oxford: Pergamon, 1984.

35. Neumann, M., *J. Chem. Phys.*, 1986, vol. 85, p. 1567.

36. Angell, C.A. and Rodgers, V., *J. Chem. Phys.,* 1984, vol. 80, p. 6245.

37. Ocana, M., Fornes, V., Garcia-Ramos, J.V., and Serna, C.J., *Phys. Chem. Miner.,* 1987, vol. 14, p. 527.

38. Goggin, P.L. and Carr, C., *Far Infrared Spectroscopy and Aqueous Solutions. Water and Aqueous Solutions*, Bristol-Boston: Adam Hilger, 1986, vol. 37, p. 149.

39. Murphy, W.F., *J. Chem. Phys.*, 1977, vol. 67, p. 5877.

40. Miler, M., *Zh. Fiz. Khim.*, 1968, vol. 18, p. 354.

41. Skolunov, A.V., *Fibre Chem.*, 1997, vol. 29, p. 367.